Cavity-Laser Stablization and Absolute Light Freuqnecy Measurement Based On Superhetrodyne Dual frequency Modulation Technique

Chenyuan Li
hyperblazor@gmail.com
Department of Physics, Harvard University

Abstract: In this lab note, we propose a new scheme for cavity-laser stabilization to achieve absolute light frequency measurements with improved accuracy compared to a commercial wavemeter, and at relatively low cost. Our method involves using a single laser, a high finesse cavity, and a microwave frequency standard to convert stability in terms of microwave frequency to light frequency. Through experimental demonstration using the superheterodyne dual frequency modulation technique (DFM), we were able to lock a laser to a cavity mode and, at the same time, measure the free spectral range (FSR) of the cavity with tens of Gigahertz sidebands. Our error signal of the superheterodyne DFM showed a fractional sensitivity of 6 parts in 10^{11}. We then calibrated the relationship between FSR and absolute light frequency, and were able to measure absolute light frequency with accuracy similar to, or perhaps better than, that of a wavemeter with 1MHz resolution. However, further comparison is necessary to determine if there is a long-term drift in the superheterodyne DFM system itself.

1 Introduction

The Pound Drever Hall (PDH) technique is commonly used in modern AMO physics to stabilize laser frequency to an optical cavity mode. However, to achieve long-term stabilization of the laser frequency, a costly Ultra-low Expansion (ULE) cavity that is well isolated in a vacuum chamber is typically required. In this lab note, we present a technique based on PDH to measure the cavity free spectral range (FSR) $c/2L$ with high precision in real-time. This enables the absolute frequency of the laser to be measured. If the long-term drift in the cavity length is compensated in an appropriate manner, this technique could enable the acquisition of an absolute optical frequency reference, and it only requires an ordinary high finesse Fabry–Pérot cavity.

This lab note is based on an idea proposed nearly four decades ago by DeVoe and Brewer[1]. The key idea of this technique is to measure the mode spacing $c/2L$ of a cavity and compare it to a radio frequency (RF) frequency standard. Once the laser is locked to one cavity mode and the cavity FSR ω_{FSR} is known, the laser absolute frequency ω_l can be calculated using the formula,

$$\omega_l/\omega_{FSR} = q + \Delta \tag{1}$$

where q is a integer mode number and Δ is a phase-shift correction. *

*For the $TEM_{n'n}$ Gaussian modes, the transverse mode frequency is,

$$\omega_{qn'n} = \frac{c}{2L}\left[q + \frac{1}{\pi}(n' + n + 1)\cos^{-1}\sqrt{g_1 g_2}\right] \tag{2}$$

where $2L$ is round trip distance q, n' and n are mode numbers. The second term in the bracket is due to the Gouy phase of Gaussian beams. $g_{1,2} = 1 - \frac{L}{R_{1,2}}$, and $R_{1,2}$ are the radius of mirrors.

In DeVoe and Brewer's dual frequency modulation (DFM) scheme, laser is phase modulated at dual frequencies. One modulation is used to lock the laser to a cavity mode using conventional PDH technique, while the other modulation, in the gigahertz range and close to an integral multiple of the cavity FSR $c/2L$, probes the nearby cavity modes. After demodulation, a PDH-like error function of the frequency difference between the cavity FSR and the high modulation frequency is obtained.

Methods based on similar idea of detecting and stabilizing cavity FSR are proposed[2, 3]. However, the fractional uncertainty of their FSR readout is so large that when converted to accuracy in absolute frequency measurement, the performance is much worse than that of a commercial wavemeter.

Previous works of DFM all use the adjacent cavity mode for FSR detection[1, 4, 5]. In order to get a better sensitivity in terms of the FSR measurement, we go to a very high modulation frequency of 12GHz, which is 8 times of our 1.5GHz cavity FSR. Because the shape of FSR error signal is only determined by the cavity linewidth, m multiple of modulation frequency gives m times of sensitivity. To obtain a high signal to noise ratio of FSR error signal, we designed a new superhetrodyne DFM scheme, where the 12GHz FSR signal is firstly down-converted to lower frequency in tens of Megahertz, allowing us to demodulate the signal and achieve a fractional sensitivity of 6 parts in 10^{11} in terms of FSR measurement.

Our open-loop FSR measurement without feedback to the cavity FSR allowed us to calibrate the relationship between the FSR and the absolute light frequency. Through our experiments using the superheterodyne DFM scheme, we found that we could accurately measure the absolute light frequency within a period of one hour with an accuracy similar to, or even better than, that of a wavemeter with a 1 MHz resolution. However, when we compared our results with the wavemeter over an 18-hour period, we found a larger deviation with a maximum difference of 2.55MHz. This indicates the need for further investigation to determine whether there is a long-term drift in the superheterodyne DFM system itself.

2 Principle of the DFM for Probing FSR

In the dual frequency modulation (DFM) technique, the laser is phase-modulated at two frequencies: ω_1 and ω_2. In this context, we refer to ω_2 (which is typically in the tens of megahertz range) as the PDH modulation frequency and to ω_1 (which is typically in the several gigahertz range) as the FSR modulation frequency. For simplicity, let us assume that the laser is already perfectly locked to the q-th cavity mode using the conventional PDH technique [6, 7]. The detuning of the FSR modulation sidebands from the nearest $(q \pm m)$-th cavity modes is denoted as $\delta = \omega_1 - m\omega_{FSR}$, where ω_{FSR} is the free spectral range of the cavity.

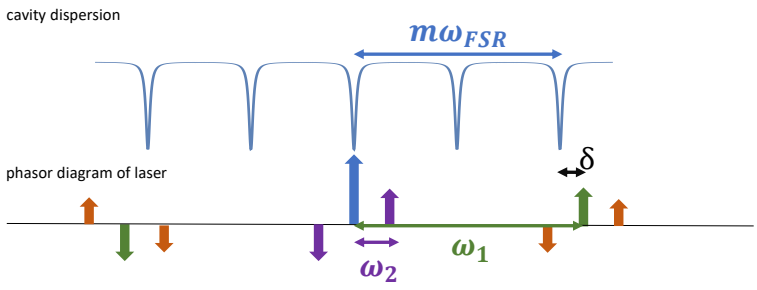

Figure 1: Laser sidebands of dual frequency modulation and their relationship to the cavity modes.

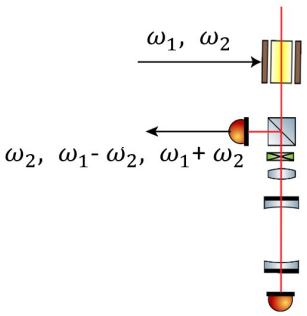

Figure 2: Schemaics of the optics and cavity's response to dual frequency modulation.

The incident light wave to the cavity can be written as:

$$E_i = E_0 \exp(i\omega_0 t) \exp(i\beta_1 \sin(\omega_1 t) + i\beta_2 \sin(\omega_2 t)) \tag{3}$$

where ω_0 is the central frequency of the laser and β_1 and β_2 are the modulation depths of the respective frequencies. Expand Eq. 3 into Fourier series using the formula,

$$\exp(i\beta_1 \sin(\omega_1 t)) = \sum_{n=-\infty}^{+\infty} J_n(\beta) e^{i\omega_1 t} \simeq J_0(\beta_1) + J_1(\beta_1)\exp(i\omega_1 t) - J_1(\beta_1)\exp(-i\omega_1 t) \tag{4}$$

$J_n(\beta)$ is the Bessel series. The property $J_{-n}(\beta) = (-)^n J_n(\beta)$ is used. Eq.3 can be written as,

$$\begin{aligned} E_i = E_0 \exp(i\omega_0 t)\Big\{ & J_0(\beta_1)J_0(\beta_2) + J_1(\beta_1)J_0(\beta_2)(e^{i\omega_1 t} - e^{-i\omega_1 t}) + J_0(\beta_1)J_1(\beta_2)(e^{i\,\omega_2 t} - e^{-i\omega_2 t})\Big\} \\ & + J_1(\beta_1)J_1(\beta_2)\left(e^{i(\omega_1+\omega_2)t} + e^{-i(\omega_1+\omega_2)t} - e^{i(\omega_1-\omega_2)t} - e^{-i(\omega_1-\omega_2)t}\right)\Big\} \end{aligned} \tag{5}$$

We only keep the Bessel series to the second order. For every frequency component ω of the incident light, the reflected light wave from the cavity at ω has the form of

$$E_r(\omega) = g(\Delta)E_i(\omega) \tag{6}$$

where Δ is the sideband ω 's detuning from its closest cavity mode, $\Delta = \omega - \omega_{Cavity\ Mode}$. Suppose cavity lineshape function $g(\Delta)$ is a Lorentzian centered at the closest cavity mode,

$$g(\Delta) = \frac{\Delta(\Delta - i\Gamma)}{(\Delta^2 + \Gamma^2)} \tag{7}$$

Γ corresponds to the cavity linewidth. Then we have,

$$\begin{aligned} E_r = & E_0 \exp(i\omega_0 t)\Big\{ g(0)J_0(\beta_1)J_0(\beta_2) + J_1(\beta_1)J_0(\beta_2)\left(g(\delta)e^{i\omega_1 t} - g(-\delta)e^{-i\omega_1 t}\right) \\ & + J_0(\beta_1)J_1(\beta_2)\left(g(\omega_2)e^{i\omega_2 t} - g(-\omega_2)e^{-i\omega_2 t}\right) \\ & + J_1(\beta_1)J_1(\beta_2)\left(g(\delta+\omega_2)e^{i(\omega_1+\omega_2)t} + g(-\delta-\omega_2)e^{-i(\omega_1+\omega_2)t} - g(\delta-\omega_2)e^{i(\omega_1-\omega_2)t} - g(-\delta+\omega_2)e^{-i(\omega_1-\omega_2)t}\right)\Big\} \end{aligned} \tag{8}$$

Note that $g(-x) = g^*(x)$, $g(0) = 0$, and for $\Delta \gg \Gamma, g(\Delta) \to 1$. The reflected light intensity is $I = E_r^* E_r$. We have,

$$\begin{aligned} I_r = E_0^* E_0 \Big\{ & \left(2\left(J_1(\beta_1)J_0(\beta_2)\right)^2 g^*(\delta)g(\delta) + 2\left(J_0(\beta_1)J_1(\beta_2)\right)^2 g^*(\omega_2)g(\omega_2)\right) \\ & + J_0(\beta_1)J_1(\beta_1)J_0(\beta_2)J_1(\beta_2)\left(g(\delta)g(\omega_2)e^{i(\omega_1+\omega_2)t} + g^*(\delta)g^*(\omega_2)e^{-i(\omega_1+\omega_2)t}\right. \\ & \left. + g(\delta)g^*(\omega_2)e^{i(\omega_1-\omega_2)t} + g^*(\delta)g(\omega_2)e^{-i(\omega_1-\omega_2)t}\right) + \ldots\Big\} \end{aligned} \tag{9}$$

In I_r, we only consider frequency components at $\omega_1 \pm \omega_2$ and omit terms with higher frequencies, as they do not affect the measurement. Eq. 9 contains no components at the frequency of ω_1 because the laser is locked to the zero-crossing point of the PDH error signal, where the amplitude of first-order terms of both frequencies ω_2 and ω_1 simultaneously goes to zero. Intuitively, all the oscillating parts in I_r arise from the beatnote of two different components in Eq. 8 or Figure 1. Ideally, because the component at the center carrier frequency is totally transmitted, in the reflected light, the amplitude of this component is 0. In Figure 1, the $\omega_1 \pm \omega_2$ components comes from the beatnote of the purple and green arrows.

3 Experimental Setup of Superheterodyne DFM Scheme

To measure FSR using the DFM scheme, accurate and stable measurements of the components of $\omega_1 + \omega_2$ or $\omega_1 - \omega_2$ in Eq. 9 are required. We use a superheterodyne detection method to obtain the FSR error signal. For this purpose, we designed a superheterodyne DFM experimental setup that operates at a frequency of 12 GHz.

Normally, the phase and amplitude of an oscillating signal in megahertz regime can be determined using homodyne detection, where the signal of interest is multiplied with another signal at the same frequency using a mixer. The output of the mixer is a DC voltage, i.e., the error signal, which is related to the relative phase and amplitude of the oscillating signal.

However, conventional homodyne detection is not suitable for our purposes because we encountered an unstable DC bias in the error signal. Microwave signals at frequencies of several gigahertz or higher are prone to leakage and picking up in unwanted places, making it challenging to maintain phase stability in such systems. When using a microwave mixer, part of the driving signal from the local oscillator (LO) port leaks to the radio frequency (RF) port. This leaked signal is then back-reflected to the RF port, creating a DC bias at the intermediate frequency (IF) port. This bias is unstable due to its sensitivity to phase shifts and impedance mismatches in the RF port. Moreover, modulation leaks to the air and is picked up by the fast fiber photo detector and the microwave amplifier at the detection side, which further deteriorates the stability of the error signal. Therefore, we decided to use the superheterodyne detection method instead.

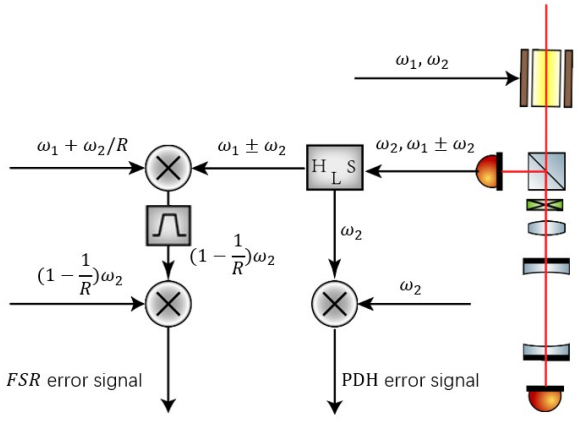

Figure 3: Frequencies involved in the superhetrodyne DFM scheme. A sum signal of ω_1 and ω_2 modulates a fiber EOM. The PD detects the modulated back-reflected light with the frequencies of ω_2 and $\omega_1 \pm \omega_2$. The high frequency and low frequency parts are separated by a diplexer. For the low frequency part, direct demodulation of ω_2 leads to the conventional PDH error signal. For the high frequency part, the signal firstly mix with signal at $\omega_1 + \omega_2/R$, where R is a constant factor. This generates down-converted signal at the frequency of $(1 \pm 1/R)\omega_2$. A bandpass filter is then applied to remove all the frequency components except $(1 - \frac{1}{R})\omega_2$. Finally, the $(1 - 1/R)\omega_2$ component is mixed with a signal at the same frequency to generate the FSR error signal. It should be noted that maintaining phase coherence between all signals involved is essential.

In our Superheterodyne DFM scheme, the FSR signal is first mixed with another signal at a nearby frequency. The resulting down-converted signal at the difference frequency between these two signals is then demodulated. This is because signals at Megahertz frequencies are much easier to manipulate and process than signals at Gigahertz frequencies.

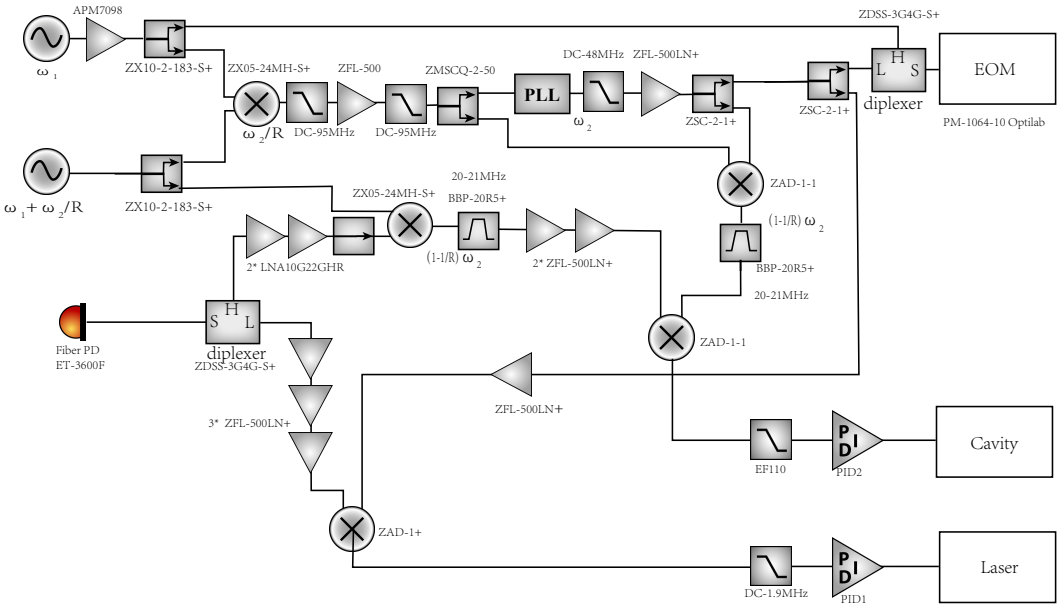

Figure 4: Block diagram of the superheterodyne DFM scheme.

In our experimental setup, we use light with a wavelength of 1062 nm and an optical cavity with a length of 10cm. The Finesse of the cavity was measured to be 1.4×10^5 using cavity ring-down measurement. The cavity was scavenged from another experiment and is an ultra-low expansion (ULE) cavity, but its further specifications are unknown. Due to changes in temperature and air pressure, the cavity FSR drifts slowly over time in our measurements.

In the Block Diagram Figure 4, microwave signals at frequencies ω_1 and $\omega_1 + \omega_2/R$ are generated by a two-channel signal generator (Windfreak SynthHD) referenced to a GPS frequency reference with a stability better than 10^{-11}. The frequencies ω_2/R, ω_2, and $(1 - 1/R)\omega_2$ are subsequently synthesized phase-coherently by multiple mixers and a Phase-Locked Loop (PLL) ADF4351. The PLL is configured to set the frequency ratio of its output and input R to $\frac{3}{2}$. The frequency ω_2 is designed to be ~ 60 MHz in order to provide adequate separation between the sidebands at the intermediate frequency after down-conversion. In order to filter out any unwanted sidebands, narrow bandpass filters with a center frequency of $(1 - 1/R)\omega_2 \sim 20$ MHz are used. The filters ensure that only the desired frequency is passed through and the unwanted signals are attenuated.

This proposed system involves two servo loops. PID1 is for PDH laser locking, while PID2 is designed for feeding back to the cavity length based on FSR error signal. (Servo to FSR is experimentally implemented in a different way as a proof of principle test, but not shown in this lab note.) In our experimental setup, the Output of PID1 is connected to both a fiber AOD driver and the internal modulation port of the NKT laser. The fiber AOD provides fast feedback to the laser frequency, while the internal modulation allows slowly compensating larger frequency drifts. Meanwhile, the PID2 is a digital one based on a National Instruments DAQ card and a LabView PID program. Absolute light frequency ω_l can be calculated and read out based on Equation $\omega_l = (q + \Delta)\omega_{FSR}$. Determining the values of q and Δ requires calibration .

4 FSR Measurement and the Error Signal

In the following section, experimental results are presented, starting with the measurement of cavity mode spacing at different multiples of the FSR. The laser is locked to one of the TEM_{00} fundamental mode of the cavity. When the FSR modulation frequency resonate with mode spacing such that the laser sidebands match perfectly with other cavity modes, the oscillating terms containing $g(\delta)$ in Eq. 9 goes to zero, resulting in the oscillation amplitude of $\omega_1 \pm \omega_2$ going to zero as well. By directly monitoring the output of the PD using a spectrum analyzer and tuning the FSR modulation frequency ω_1, resonant frequencies are found and listed in Table 1. The resonant frequency is linear with m, while the ω_{FSR} remains constant and agrees with each other to the 10th digit. It should be noted that the measurement in Table 1 is conducted manually point by point over a period of ~ 30 minutes, and the FSR is subject to drift during this time, which limits the comparison of ω_{FSR} to higher accuracy.

m	**Resonant Frequency (GHz)**	ω_{FSR}**(GHz)**
13	19.488364827	1.4991049867
12	17.989259829	1.4991049858
11	16.490154838	1.4991049853
10	14.991049836	1.4991049836
9	13.491944859	1.4991049843
8	11.992839875	1.4991049843
7	10.493734892	1.4991049846

Table 1: Measured Cavity FSR. When the FSR modulation frequency ω_1 is tuned to the m multiples of the FSR, the resonant frequency is read out through a spectrum analyzer looking at the peaks of $\omega_1 \pm \omega_2$.The FSR is calculated by ω_{FSR}=Resonant Frequency/m. ω_{FSR} agrees with each other to the 10th digit.

Parameter	Experimental Value
signal generator Channel 0 power(ω_1)	20 dBm (unleveled)
signal generator Channel 1 power($\omega_1 + \omega_2/R$)	20 dBm (unleveled)
channel frequency difference ω_2/R	43.09MHz
PLL Ratio R	$\frac{3}{2}$
Cavity Finesse	14000
Cavity FSR	1.499105 GHz

Table 2: Experimental parameters for FSR measurement

Next, we implemented the superheterodyne DFM scheme shown in the block diagram of Figure 4. We measured the FSR error signal using this setup, as shown in Figure 5, with the experimental parameters listed in Table 2. The data was obtained by scanning ω_1 and measuring the FSR error signal voltage using an NI DAQ.

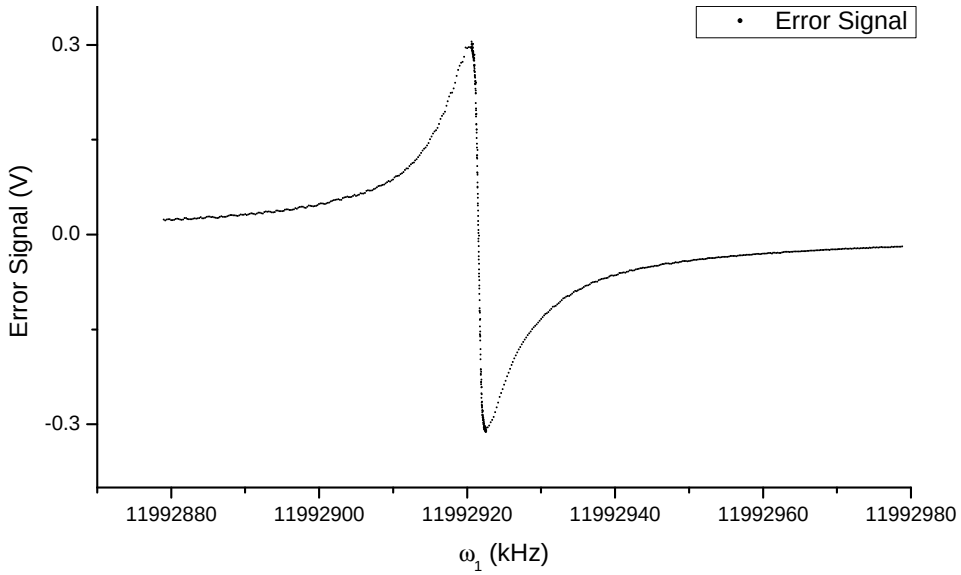

Figure 5: FSR error signal. Measured by scanning ω_1 across the resonant point at $8\omega_{FSR} \sim 12GHz$, ω_2 is fixed at 43.09 MHz. The data is taken point by point with a 10Hz spacing at the center.

The slope of the error signal at the zero point was found to be $-0.6\,\mathrm{mV/Hz}$, and the noise of a data point was 0.8 mV (rms, averaged for 1s). Based on this, the fractional sensitivity of FSR measurement was estimated to be about 6 parts in 10^{11}. If we directly translate this to sensitivity in terms of light frequency, it corresponds to approximately $\sim 18\,\mathrm{kHz}$.

5 Comparison with Wavemeter and the Long-term Performance

Then we compare the superheterodyne DFM readout with a HighFinesse WS7 wavemeter, which is referenced to a iodine clock. (The iodine clock is a NPRO laser at 1064nm, whose frequency is doubled and locked to the iodine R56(32)-0 transition at 532nm. It has a stability of $\sim 1\,\mathrm{kHz}$[8]). We calibrate the relationship of absolute light frequency ω_l and free spectral range ω_{FSR}. To conduct a open-loop FSR measurement for calibration and comparison, the system is built as the block diagram shown in Figure 4, except that no feedback is applied to the cavity. The light frequency changes with the drifting in cavity FSR.

By scanning the FSR modulation frequency ω_1 across the FSR error signal zero point $\omega_{resonant}$ at a frequency of 8 times the FSR, we obtain $\omega_{FSR} = \omega_{resonant}/8$. A scanning is conducted in the region of $\omega_{resonant} \pm 1000\,\mathrm{Hz}$, with 200 data points. One data point is the mean value of 20 measurements of voltage. The scanning region is self-adapting based on the former measurement $\omega'_{resonant}$ so that the zero-crossing point is always in the scanning region. Occasionally, if the cavity drifts too fast and a zero-crossing point cannot be found during a scan, the previous scanning is discarded, and a larger region is scanned instead. The system can complete about 3 normal scanning every minute.

In our data analysis and calibration, we assumed that the cavity drifts much slower than the period of one scanning. (However, further analysis revealed that this was not always the case.) At the beginning and the end of each scanning, we readout the light frequency using the wavemeter, denoted as $\omega_{l,w}^{before}$ and $\omega_{l,w}^{after}$, respectively. We take the mean value of these two readings as the light frequency $\omega_{l,w} \coloneqq (\omega_{l,w}^{before} + \omega_{l,w}^{after})/2$ for calibration and comparison.

We continuously took measurements over a time period of 18 hours and used these data to fit a linear function between ω_{FSR} and the light frequency $\omega_{l,w}$. The linear function is given by

$$\omega_{l,w} = a \cdot \omega_{FSR} \tag{10}$$

where a is the fitted coefficient and is found to be $a = 188319.37806349$. To validate the accuracy of

the superheterodyne DFM light frequency readout, we compared it with the wavemeter readout $\omega_{l,w}$, as shown in Figure 6.

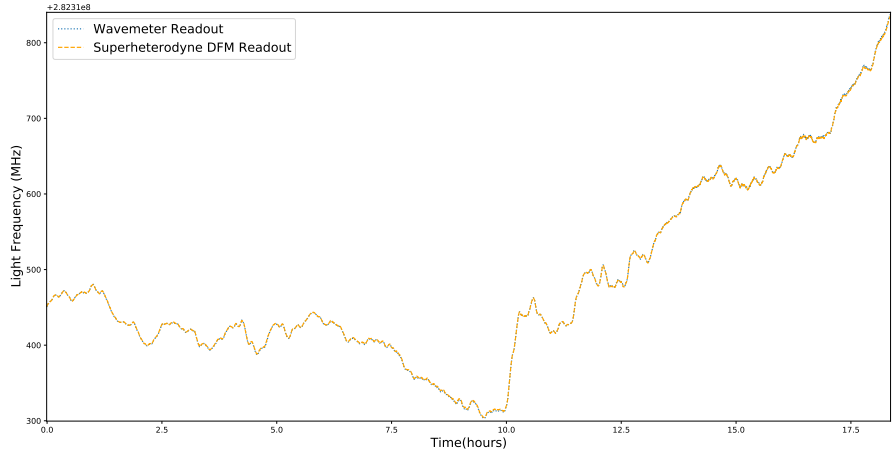

Figure 6: Comparsion between Superheterodyne DFM readout and a wavemeter readout over ∼18 hours.

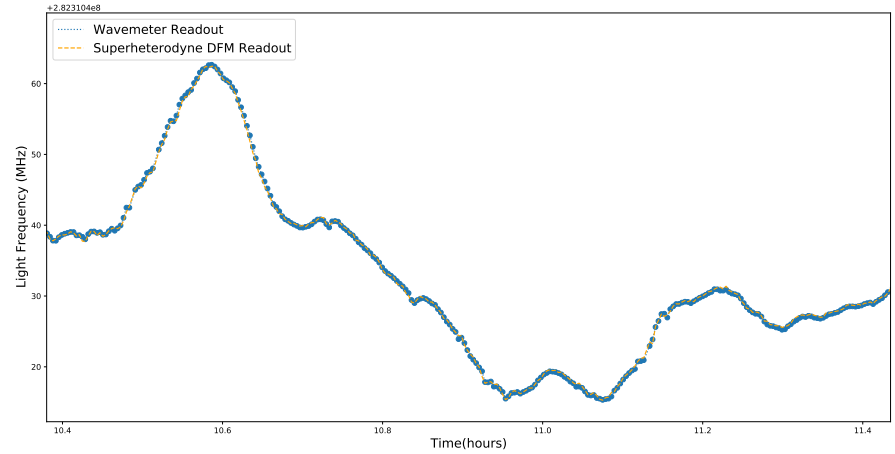

Figure 7: A zoomed-in view of the data in Figure 6 comparison over ∼ 1 hours. It is in a selected time region where the difference between two methods is relatively small.

Over the measuring period of 18 hours, the light frequency drift for about 500MHz due to drifts in cavity. As shown in Figure 6 and 7, the superheterodyne DFM $\omega_{l,DFM}$ readout follows the dirft in light frequency measured by wavemeter. We evaluate the long term performance by camparing two readouts, shown in Table 3.

Interestingly, we found that during periods of relatively slow cavity drift rates (as shown in the zoomed-in region of Figure 7), the maximum value and standard deviation of the difference between the two readouts $(\omega_{l,DFM} - \omega_{l,w})$ were even smaller than those of the wavemeter readings themselves $(\omega_{l,w}^{before} - \omega_{l,w}^{after})$. This suggests that the wavemeter measurement may not be accurate enough to fully evaluate the accuracy of the superheterodyne DFM. This could be due to two factors: the first being that the WS7 has an uncertainty of about 700 kHz when compared with the iodine clock, and the second being that the wavemeter measurement is conducted at the beginning and end of each DFM error signal scanning, during which the cavity drifts. In contrast, the $\omega_{l,DFM}$ readout is closer to the cavity resonant frequency at the middle time of the measurement, which is closer to the mean value of $\omega_{l,w}^{before}$ and $\omega_{l,w}^{after}$,

assuming that drift is linear in the scanning period.

18 hours comparison	Value (kHz)	1 hour comparison (selected region)	Value (kHz)
$max\{\left\|\omega^i_{l,w} - \omega^i_{l,DFM}\right\|\}$	2551	$max\{\left\|\omega^i_{l,w} - \omega^i_{l,DFM}\right\|\}$	569
$max\{\left\|\omega^{before}_{l,w} - \omega^{after}_{l,w}\right\|\}$	3889	$max\{\left\|\omega^{before}_{l,w} - \omega^{after}_{l,w}\right\|\}$	2536
$\overline{(\omega^i_{l,w} - \omega^i_{l,DFM})}$	-0.038	$\overline{(\omega^i_{l,w} - \omega^i_{l,DFM})}$	-27.2
$std\left(\omega^i_{l,w} - \omega^i_{l,DFM}\right)$	689	$std\left(\omega^i_{l,w} - \omega^i_{l,DFM}\right)$	181
$std\left(\omega^{before}_{l,w} - \omega^{after}_{l,w}\right)$	347	$std\left(\omega^{before}_{l,w} - \omega^{after}_{l,w}\right)$	337

Table 3: Evaluation of long term performance of superhetrodyn DFM scheme. Superhetrodyne DFM light frequency readout $\omega_{l,DFM}$ is compared with wavemeter light frequency readout $\omega_{l,w}$ over time periods of 18 hours and an hour, using the data shown in Figure 6 and 7. $std\left(\omega^i_{l,w} - \omega^i_{l,DFM}\right) = \sqrt{\overline{(\omega^i_{l,w} - \omega^i_{l,DFM})^2} - \left(\overline{\omega^i_{l,w} - \omega^i_{l,DFM}}\right)^2}$, $std\left(\omega^{before}_{l,w} - \omega^{after}_{l,w}\right) = \sqrt{\overline{(\omega^{before}_{l,w} - \omega^{after}_{l,w})^2} - \left(\overline{\omega^{before}_{l,w} - \omega^{after}_{l,w}}\right)^2}$

However, over the entire 18-hour period, a larger deviation between the two measurement methods was observed. Figure 8 shows the frequency difference between the two methods, and it is evident that the deviation is not solely due to noise but possibly due to systematic errors. In some time region like that of Figure 7, the deviation between the two methods is relatively small. but in other regions, it is larger. The largest difference is 2.55 MHz, though still smaller than the maximum value of $\omega^{before}_{l,w} - \omega^{after}_{l,w}$. Possible explanations include the cavity drifting too quickly during one scanning interval. And the averaged wavemeter readout $\omega_{l,w} = (\omega^{before}_{l,w} + \omega^{after}_{l,w})/2$ deviates from the laser frequency when the scanning goes through the zero-crossing point. Additionally, there may be long-term drifts in the superheterodyne DFM system due to temperature changes affecting the microwave relative phase in the microwave cables, causing the error signal to change its shape, although in this scheme the zero point is not sensitive to relative microwave phase to the first order.

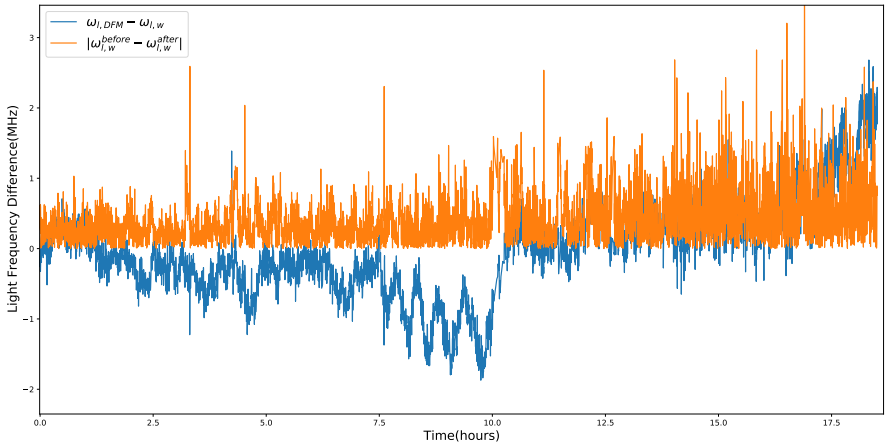

Figure 8: The frequency difference of two ways of readouts.

Further investigation is needed to determine the underlying cause of the larger deviation and to identify if there is a drift in Superheterofyne DFM system itself.

6 Discussion and Conclusion

In conclusion, We have demonstrated a new scheme of superheterodyne dual frequency modulation for measuring cavity free spectral range. By operating at a high modulation frequency of 12GHz and im-

plementing a detection scheme with high signal to noise ratio, we obtain a error signal for measuring free spectral range ω_{FSR} with fractional sensitivity of 6 parts in 10^{11}. Then we demonstrated that ω_{FSR} can be converted to absolute light frequency after calibration. The absolute light frequency readout of superheterodyne DFM has comparable stability with a WS7 wavemeter. During a 18 hours comparison, the RMS of the difference of two methods of readout is $\sim 700\,\mathrm{kHz}$. During a hour when the cavity drifting is relatively slow the RMS of the difference is $\sim 200\,\mathrm{kHz}$. It is at the same scale with the resolution of wavemeter. However, we do observe a long-term deviation in our 18 hour comparison. The peak-to-peak difference of Superheterodyne DFM readout and the wavemeter readout is 2.55MHz in the 18 hours. Whether it is caused by the Superhetrodyne DFM itself, or by the fast drifting in the cavity FSR and the inaccurate wavemeter readout is unknown and needs further investigation.

As a proof of principle experiment, the cavity we used is a ULE cavity in air, which limited our ways of feedback to cavity length. We have already tried to feedback to the cavity FSR by adjusting air pressure in the cavity (by pushing a membrane on the hole on cavity's side using a rod attached to a voice coil).Preliminary results showed successful stabilization of the cavity FSR for several minutes, although these results are not included in this note.

In future work, if cavity is sealed in a chamber so that the cavity FSR drift is slow, better calibration might been done. With the demonstrated FSR measurement sensitivity, the superheterodyne DFM could potentially achieve 1-2 orders of magnitude higher accuracy than state-of-the-art commercial wavemeters in terms of absolute frequency measurement and laser locking. If a carefully designed and fabricated cavity is used, it may be possible to calculate the phase-shift correction Δ using Eq. 2 and compare it with the calibrated result. It should be noted that in Ref. [5], a different DFM scheme was implemented. Their DFM light frequency readout was heterodyne beatnoted with a laser locked to a narrow iodine transition for comparison, demonstrating a 2.5MHz long-term peak-to-peak absolute frequency change of FSR readout. Due to the higher FSR readout sensitivity demonstrated by our superheterodyne DFM scheme, it is likely to show even better performance with future improvements and stringent comparison.

If a cavity is carefully designed and fabricated to minimize FSR drift, it may be possible to calculate the phase-shift correction Δ using Eq. 2 and compare it with the calibrated result. Notably, in Ref. [5], a different DFM scheme was implemented, with their DFM light frequency readout heterodyne beatnoted with a laser locked to a narrow iodine transition for more accurate comparison, demonstrating a 2.5MHz long-term peak-to-peak absolute frequency change of FSR readout. Due to the higher FSR readout sensitivity demonstrated by our superheterodyne DFM scheme, it is likely to show even better performance with future improvements and rigorous comparison.

Acknowledgments

This project was completed under the instruction of Yicheng Bao. The experiment was primarily conducted by Chenyuan Li, when he served as a visiting undergraduate research fellow in Prof. John Doyle's group at Harvard. The experiment is made possible by equipments provided by the CaF Generation 2 experiment. The author expresses gratitude to Prof. John Doyle and Yicheng Bao for their guidance and many people in Doyle group for their thoughtful discussions. Chenyuan Li acknowledges the Tsinghua Xuetang Program for providing stipend during his internship.

References

[1] R. G. DeVoe and R. G. Brewer. Laser-frequency division and stabilization. *Phys. Rev. A*, 30:2827–2829, Nov 1984.

[2] Gaëtan Hagel, Marie Houssin, Martina Knoop, Caroline Champenois, Michel Vedel, and Fernande

Vedel. Long-term stabilization of the length of an optical reference cavity. *Review of scientific instruments*, 76(12):123101, 2005.

[3] Masato Aketagawa, Takuya Yashiki, Shohei Kimura, and Tuan Quoc Banh. Free spectral range measurement of fabry-perot cavity using frequency modulation. *International Journal of Precision Engineering and Manufacturing*, 11:851–856, 2010.

[4] Emily Rose Rees, Andrew R Wade, Andrew J Sutton, Robert E Spero, Daniel A Shaddock, and Kirk Mckenzie. Absolute frequency readout derived from ule cavity for next generation geodesy missions. *Optics Express*, 29(16):26014–26027, 2021.

[5] Emily Rose Rees, Andrew R Wade, Andrew J Sutton, and Kirk McKenzie. Absolute frequency readout of cavity against atomic reference. *Remote Sensing*, 14(11):2689, 2022.

[6] R. W. P. Drever, J. L. Hall, F. V. Kowalski, J. Hough, G. M. Ford, A. J. Munley, and H. Ward. Laser phase and frequency stabilization using an optical resonator. *Applied Physics B Photophysics and Laser Chemistry*, 31(2):97–105, 1983.

[7] Eric D. Black. An introduction to pound–drever–hall laser frequency stabilization. *American Journal of Physics*, 69(1):79–87, 2001.

[8] Daniel Farkas. *An optical reference and frequency comb for improved spectroscopy of helium*, volume 68. 2006.